

## A. APPENDIX

### A.1. FEA

This section as background on the analysis methods, element types and software used. Finite element analyses are often treated on a parametric basis in academic discussions. This is possible for the treatment of relatively simple problems where the finite element discretization can be quantified (the exact divisions can be shown and listed in a simple geometry). For such cases, the finite element formulation can be printed to the detail of the exact geometric co-ordinates of nodes, numerical calculation and values in the stiffness matrix, nodal loads etc.

The dissertation deals with an actual analysis case of a complex geometry and relies on the experience and skills of the analyst to ensure convergence of the finite element mesh, appropriate discretization, solver routines etc. The results can be reproduced with a small numerical deviation by any competent analyst, if the same assumptions are used, without direct knowledge of the exact location of nodes, number of elements, or even element types.

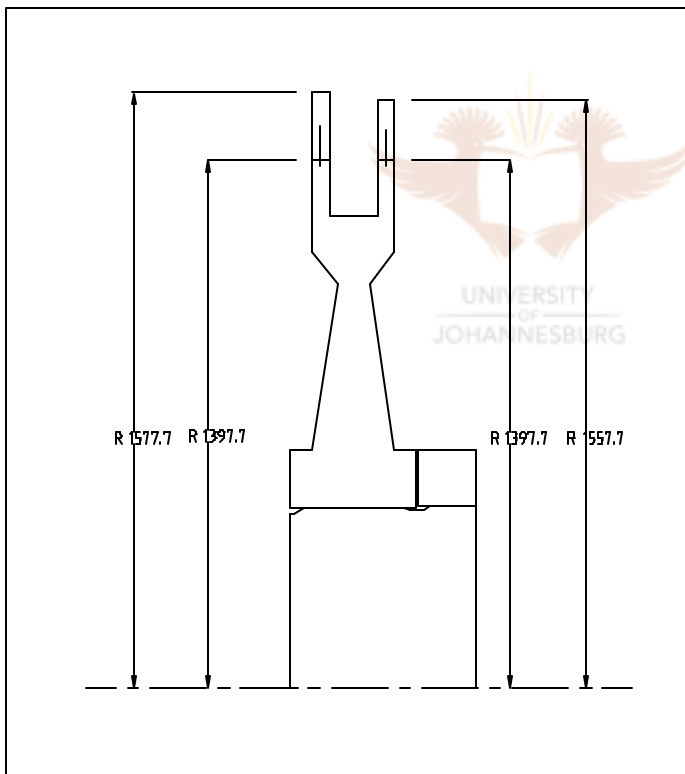


Figure A1: Geometry of Stage 1/2 disk and centre ring.

The finite element code, ANSYS, was used in all the analysis. All solid structural elements (2D and 3D) have quadratic shape functions. A number of contact element types are available in the ANSYS code. Point-to-point contact elements were used on the shrink surfaces.

## A.2. MODELLING OF SHRINK AND FRICTION

Figure A1 shows the basic geometry of the axi-symmetric model used. The right hand side of the section is a symmetry plane through the middle of the rotor, while the left hand side is a plane intersecting with the edge of the stage 1/2 disk.

Figure A2 shows the finite element boundary conditions that were applied. The transverse cut through the middle of the rotor is used as a symmetry plane. The assumption was made that a cut between disks 1/2 and disk 3 is also a symmetry plane, but that this plane is free to move in the axial direction as is the case for the actual rotor. The free end symmetry was modelled by coupling all nodes on this face in the axial direction i.e. the face is free to move axially but is forced to stay in the same plane.

Blade forces (see figure A1) was applied as negative pressures on the disk rim (blade attachment areas). Values of 15.1 and 18.3 MPa was calculated for stage 1 and 2 blades respectively. Disk 1/2 and the centre ring were modelled with interferences of 2.225 and 0.99 mm on the diameter respectively.

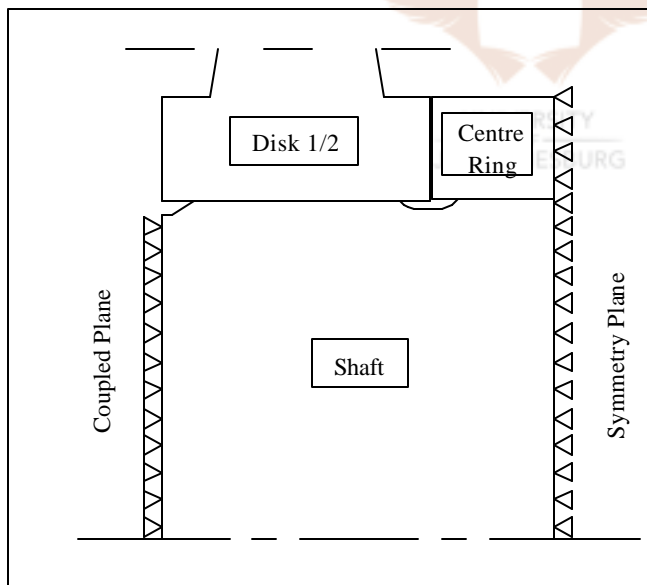


Figure A2: Finite element constraints

Non axi-symmetric features, like the keyway shown in figure 6.2 and cracks, cannot be modelled in an axi-symmetric model. Three dimensional models are used for this purpose. The basic 3D model is a direct extension of the axi-symmetric model so that the end constraints, blade forces and interferences are as described above. The

keyway and cracks were modelled as a geometrical features (as shown in figure 6.18). The nodes in crack tip elements were moved to conform to the crack tip elements described in chapter 4.

The models are also subjected to inertia loads which was applied as an angular velocity around the centre of the shaft. The body forces associated with inertia loads are calculated by ANSYS on an element volume basis.

### A.3. MODELING OF BENDING

For the purposes of calculating fracture parameters in bending, a simple shaft model was used. The shaft model has a symmetry plane at the location of the transverse crack and extends to 3 times the diameter to eliminate end effects at the crack plane.

Figure A3 shows the basic model. The bending stress,  $\sigma_b$ , was calculated from the standard formula as follows:

$$\sigma_b = \frac{My}{I}$$

where  $M$  = Bending moment of 1.2775 MN.m (see section 6.1)  
 $y$  = Distance to outer fibre of section (radius of rotor)  
 $I$  = Second moment of area.

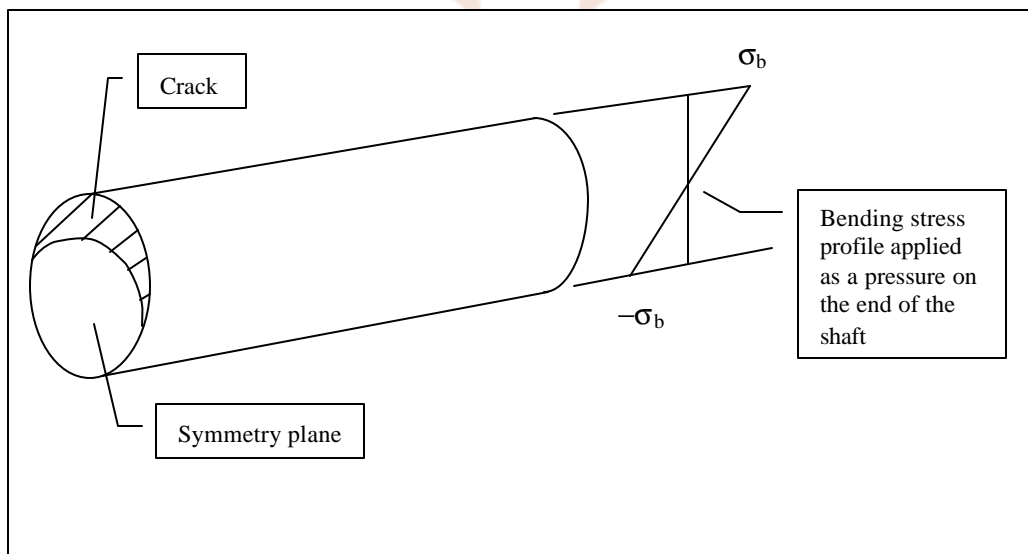


Figure A3: Model for the calculation of bending stress

The keyway was modelled where appropriate (for small cracks) to account for its stress raising effects. Table 6.5 lists the calculated  $\Delta K_I$  values and indicates models where the key was omitted by the symbol, \*.

## A.4. MODELING OF TORSION

Power is generated down the turbine train and is transmitted to the generator (see figure 6.6). The generating power distribution between turbines is given in chapter 6. The torque can be calculated by considering the power at a given speed (in this case 1500 rpm or 157.1 rad./sec) as follows:

$$[\text{Power}] = [\text{Torque}] \times [\text{Angular velocity}] = [\text{Torque}] \times [157.1]$$

Consider the middle section of LP3. The keyway region of LP3 transmits the power generated in the HP, LP1, LP2 and half the power generated in LP3 ( $298.5 + 225.2 + 225.2 + 112.6 = 861.5$  MW). The associated torque is calculated as  $861.5/157.1 = 5.48$  MN.m.

The model used for the calculation of stresses resulting from torque is similar to that of the bending model (figure A3), but extend in both directions from the crack by 3 times the shaft diameter (see figure A4).

One end of the shaft was constrained in all degrees of freedom (the fixed end). The torque was applied by calculating the force at the radius of the shaft according to:

$$[\text{Torque}] = [\text{Force}] \times [\text{Radius}]$$

The resulting force was distributed evenly between the nodes on the radius of the free end and applied as nodal loads in the tangential direction as shown in figure A4. The magnitude of the nodal loads depends on the number of nodes which are not the same for the different crack models.

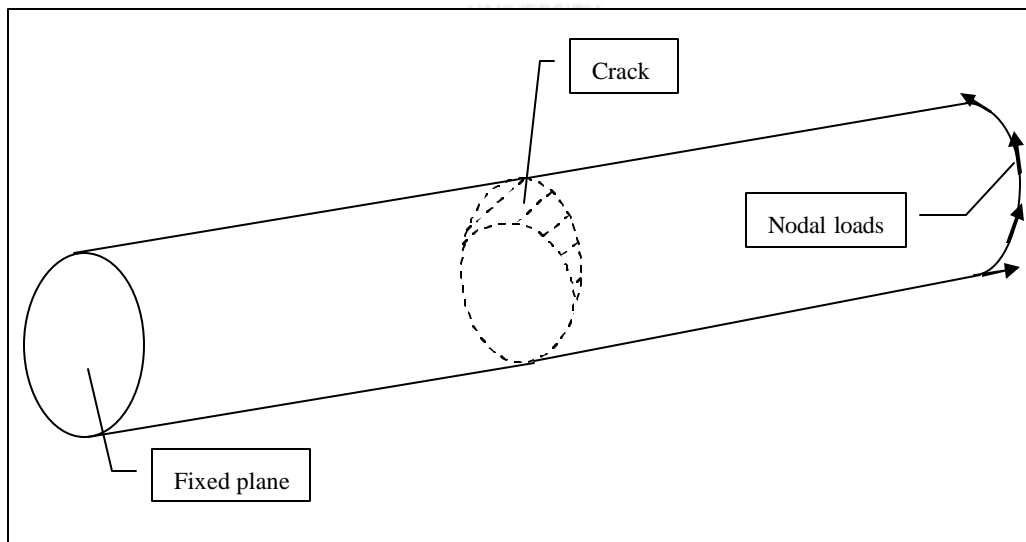


Figure A4: Model for the calculation of torsional stress